

Bulk viscosity in kaon condensed matter

Debarati Chatterjee and Debades Bandyopadhyay

Saha Institute of Nuclear Physics, 1/AF Bidhannagar, Kolkata-700064, India

Abstract

We investigate the effect of K^- condensed matter on bulk viscosity and r-mode instability in neutron stars. The bulk viscosity coefficient due to the non-leptonic process $n \rightleftharpoons p + K^-$ is studied here. In this connection, equations of state are constructed within the framework of relativistic field theoretical models where nucleon-nucleon and kaon-nucleon interactions are mediated by the exchange of scalar and vector mesons. We find that the bulk viscosity coefficient due to the non-leptonic weak process in the condensate is suppressed by several orders of magnitude. Consequently, kaon bulk viscosity may not damp the r-mode instability in neutron stars.

PACS numbers: 97.60.Jd, 26.60.+c, 04.40.Dg

I. INTRODUCTION

Astrophysical compact objects such as neutron stars and black holes, are candidates of gravitational waves. Neutron stars pulsate in different modes due to its fluid perturbation. The Coriolis restored inertial r-modes of rapidly rotating neutron stars may be sources of detectable gravitational waves. Gravitational radiation drives the r-modes unstable due to Chandrasekhar-Friedman-Schutz mechanism [1, 2, 3, 4, 5, 6, 7, 8, 9]. On the other hand, this instability may be suppressed in different ways. One plausible explanation for the damping of the instability is the large bulk viscosity coefficient due to non-leptonic processes involving hyperons [10, 11, 12, 13, 14, 15, 16]. However, it may not be an efficient damping mechanism if hyperons are superfluid [15, 17, 18]. Another possibility of damping the r-mode instability is the mutual friction between inter-penetrating neutron and proton superfluids [18, 19]. This shows that superfluidity of neutron star matter plays a significant role on the damping of the r-modes in neutron stars.

Besides hyperons, other novel phases with large strangeness fraction such as quark matter and Bose-Einstein condensed matter of K^- mesons, may appear in neutron star interior. Already the bulk viscosity of unpaired quark matter and its influence on the r-mode instability were investigated by various groups [20, 21, 22, 23]. Recently, bulk viscosity coefficients due to weak processes in quark-hadron mixed phase [14, 24] and color superconducting quark matter [25, 26, 27, 28] have been studied by several groups. However, there are no calculations of bulk viscosity in Bose-Einstein condensed matter so far.

Kaplan and Nelson [29] first demonstrated that Bose-Einstein condensation of K^- mesons in dense hadronic matter was a possibility. This calculation was performed using a chiral $SU(3)_L \times SU(3)_R$ Lagrangian. It was noted that the strongly attractive K^- -nucleon interaction lowered the effective mass and in-medium energy of K^- mesons in dense matter. The s-wave condensation sets in when the in-medium energy of negatively charged kaons equals to its chemical potential. Kaon condensation in neutron star interior was investigated extensively in the chiral [30, 31, 32, 33] and the meson exchange models [34, 35, 36, 37, 38, 39, 40, 41, 42]. The onset of K^- condensation in neutron star matter depends on the nuclear equation of state as well as on the depth of antikaon optical potential. Earlier calculations showed that kaon condensation might set in at around two times normal nuclear matter density [42]. However, the early appearance of hyperons may

delay K^- condensation to higher density or vice versa.

With the onset of K^- condensation, the neutron star matter is in chemical equilibrium through the weak process $n \rightleftharpoons p + K^-$. The density perturbation associated with the r-modes drives the system out of chemical equilibrium. The weak non-leptonic processes may reestablish the equilibrium. Therefore, it motivates us to investigate the bulk viscosity due to this non-leptonic process in kaon condensed matter and its influence on neutron star r-modes. The paper is organised in the following way. In section 2, we describe the field theoretical models of strong interactions, different phases of dense matter, the bulk viscosity coefficient and the corresponding time scale. Results of our calculation are explained in section 3. Section 4 gives summary and conclusions.

II. FORMALISM

Here we consider a first order phase transition from hadronic to K^- condensed matter in neutron stars. Both the pure hadronic and K^- condensed matter are described within the framework of relativistic field theoretical models. The constituents of matter in both phases are neutrons (n), protons (p), electrons and muons. Neutrons and protons embedded in the K^- condensate behave dynamically differently than those of the hadronic phase. It was attributed to different mean fields which nucleons experienced in the pure phases [34, 35, 42]. Local charge neutrality and beta-equilibrium conditions are satisfied in both phases. The baryon-baryon interaction is mediated by the exchange of scalar and vector mesons. Therefore the Lagrangian density for the pure hadronic phase is given by

$$\begin{aligned} \mathcal{L}_B = & \sum_{B=n,p} \bar{\psi}_B (i\gamma_\mu \partial^\mu - m_B + g_{\sigma B} \sigma - g_{\omega B} \gamma_\mu \omega^\mu - g_{\rho B} \gamma_\mu \mathbf{t}_B \cdot \boldsymbol{\rho}^\mu) \psi_B \\ & + \frac{1}{2} (\partial_\mu \sigma \partial^\mu \sigma - m_\sigma^2 \sigma^2) - U(\sigma) \\ & - \frac{1}{4} \omega_{\mu\nu} \omega^{\mu\nu} + \frac{1}{2} m_\omega^2 \omega_\mu \omega^\mu - \frac{1}{4} \boldsymbol{\rho}_{\mu\nu} \cdot \boldsymbol{\rho}^{\mu\nu} + \frac{1}{2} m_\rho^2 \boldsymbol{\rho}_\mu \cdot \boldsymbol{\rho}^\mu . \end{aligned} \quad (1)$$

Here ψ_B denotes the Dirac bispinor for baryons B with vacuum mass m_B and the isospin operator is \mathbf{t}_B . The scalar self-interaction term [43] is

$$U(\sigma) = \frac{1}{3} g_2 \sigma^3 + \frac{1}{4} g_3 \sigma^4 . \quad (2)$$

We perform this calculation in the mean field approximation [44]. The mean meson fields σ , ω_0 and ρ_{03} in the hadronic phase are given by

$$m_\sigma^2 \sigma = -\frac{\partial U}{\partial \sigma} + \sum_{B=n,p} g_{\sigma B} n_B^{h,S} , \quad (3)$$

$$m_\omega^2 \omega_0 = \sum_{B=n,p} g_{\omega B} n_B^h , \quad (4)$$

$$m_\rho^2 \rho_{03} = \sum_{B=n,p} g_{\rho B} I_{3B} n_B^h . \quad (5)$$

Here $n_B^{h,S}$ and n_B^h are scalar and baryon number densities in the hadronic phase.

The total charge density of the hadronic phase is

$$Q^h = \sum_{B=n,p} q_B n_B^h - n_e - n_\mu = 0 , \quad (6)$$

where q_B is the charge of baryons B in the pure hadronic phase and n_e and n_μ are charge densities of electrons and muons respectively. The β -equilibrium in this phase leads to $\mu_n^h = \mu_p^h + \mu_e$. The chemical potential for baryons B is given by

$$\mu_B^h = \left(k_{FB}^2 + m_B^{*h2} \right)^{1/2} + g_{\omega B} \omega_0 + I_{3B} g_{\rho B} \rho_{03} , \quad (7)$$

where effective baryon mass is $m_B^{*h} = m_B - g_{\sigma B} \sigma$ and isospin projection for baryons B is I_{3B} .

The energy density and pressure in this phase are given by

$$\begin{aligned} \varepsilon^h = & \frac{1}{2} m_\sigma^2 \sigma^2 + \frac{1}{3} g_2 \sigma^3 + \frac{1}{4} g_3 \sigma^4 + \frac{1}{2} m_\omega^2 \omega_0^2 + \frac{1}{2} m_\rho^2 \rho_{03}^2 \\ & + \sum_{B=n,p} \frac{2J_B + 1}{2\pi^2} \int_0^{k_{FB}} (k^2 + m_B^{*h2})^{1/2} k^2 dk + \sum_{l=e^-, \mu^-} \frac{1}{\pi^2} \int_0^{K_{Fl}} (k^2 + m_l^2)^{1/2} k^2 dk , \end{aligned} \quad (8)$$

$$\begin{aligned} P^h = & -\frac{1}{2} m_\sigma^2 \sigma^2 - \frac{1}{3} g_2 \sigma^3 - \frac{1}{4} g_3 \sigma^4 + \frac{1}{2} m_\omega^2 \omega_0^2 + \frac{1}{2} m_\rho^2 \rho_{03}^2 \\ & + \frac{1}{3} \sum_{B=n,p} \frac{2J_B + 1}{2\pi^2} \int_0^{k_{FB}} \frac{k^4 dk}{(k^2 + m_B^{*h2})^{1/2}} + \frac{1}{3} \sum_{l=e^-, \mu^-} \frac{1}{\pi^2} \int_0^{K_{Fl}} \frac{k^4 dk}{(k^2 + m_l^2)^{1/2}} . \end{aligned} \quad (9)$$

The baryon-baryon interaction in the pure kaon condensed phase has the same form as given by Eq. (1). In this case, we adopt a relativistic field theoretical approach for the description of (anti)kaon-baryon interaction [34, 35, 42]. Besides the exchange of σ , ω and ρ mesons, (anti)kaon-(anti)kaon interaction is also mediated by two strange mesons, scalar

meson $f_0(975)$ (denoted hereafter as σ^*) and the vector meson $\phi(1020)$. As nucleons do not couple with strange mesons, $g_{\sigma^*N} = g_{\phi N} = 0$. The Lagrangian density for (anti)kaons in the minimal coupling scheme is,

$$\mathcal{L}_K = D_\mu^* \bar{K} D^\mu K - m_K^{*2} \bar{K} K , \quad (10)$$

where the covariant derivative is $D_\mu = \partial_\mu + ig_{\omega K} \omega_\mu + ig_{\phi K} \phi_\mu + ig_{\rho K} \mathbf{t}_K \cdot \boldsymbol{\rho}_\mu$ and the effective mass of (anti)kaons is $m_K^* = m_K - g_{\sigma K} \sigma - g_{\sigma^* K} \sigma^*$. The mean meson fields in the condensed phase are denoted by σ , σ^* , ω_0 , ϕ_0 and ρ_{03} . The in-medium energy of K^- mesons for s -wave ($\vec{k} = 0$) condensation is given by

$$\omega_{K^-} = \mu_{K^-} = m_K^* - g_{\omega K} \omega_0 - g_{\phi K} \phi_0 + I_{3K^-} g_{\rho K} \rho_{03} , \quad (11)$$

where μ_{K^-} is the chemical potential of K^- mesons and the isospin projection is $I_{3K^-} = -1/2$. The mean fields in the K^- condensed phase are

$$m_\sigma^2 \sigma = -\frac{\partial U}{\partial \sigma} + \sum_{B=n,p} g_{\sigma B} n_B^{K,S} + g_{\sigma K} n_{K^-} , \quad (12)$$

$$m_{\sigma^*}^2 \sigma^* = \sum_{B=n,p} g_{\sigma^* B} n_B^{K,S} + g_{\sigma^* K} n_{K^-} , \quad (13)$$

$$m_\omega^2 \omega_0 = \sum_{B=n,p} g_{\omega B} n_B^K - g_{\omega K} n_{K^-} , \quad (14)$$

$$m_\phi^2 \phi_0 = \sum_{B=n,p} g_{\phi B} n_B^K - g_{\phi K} n_{K^-} , \quad (15)$$

$$m_\rho^2 \rho_{03} = \sum_{B=n,p} g_{\rho B} I_{3B} n_B^K + g_{\rho K} I_{3K^-} n_{K^-} . \quad (16)$$

The scalar and baryon number densities in the condensed phase are given by

$$n_B^{K,S} = \frac{2J_B + 1}{2\pi^2} \int_0^{k_{FB}} \frac{m_B^{*K}}{(k^2 + m_B^{*K^2})^{1/2}} k^2 dk , \quad (17)$$

$$n_B^K = (2J_B + 1) \frac{k_{FB}^3}{6\pi^2} , \quad (18)$$

where Fermi momentum is k_{FB} and spin is J_B . The effective baryon mass (m_B^{*K}) in the condensate has the same form as in the hadronic phase. In the absence of source terms for K^- mesons in Eq. (12)-(16), we retain the mean fields in the hadronic phase. The scalar density of K^- mesons in the condensate is given by [35]

$$n_{K^-} = 2 \left(\omega_{K^-} + g_{\omega K} \omega_0 + g_{\phi K} \phi_0 + \frac{1}{2} g_{\rho K} \rho_{03} \right) \bar{K} K = 2m_K^* \bar{K} K . \quad (19)$$

The total charge density in the condensed phase is

$$Q^K = \sum_{B=n,p} q_B n_B^K - n_K^- - n_e - n_\mu = 0 \quad (20)$$

With the onset of K^- condensation, we have

$$n \rightleftharpoons p + K^- . \quad (21)$$

The requirement of chemical equilibrium yields

$$\mu_n^K - \mu_p^K = \mu_{K^-} = \mu_e . \quad (22)$$

Here the baryon chemical potential has the same form as given by Eq. (7), but the mean fields used here are obtained in the presence of the condensate.

The total energy density in the kaon condensed phase is comprised of baryons, leptons and antikaons

$$\begin{aligned} \varepsilon^K = & \frac{1}{2}m_\sigma^2\sigma^2 + \frac{1}{3}g_2\sigma^3 + \frac{1}{4}g_3\sigma^4 + \frac{1}{2}m_{\sigma^*}^2\sigma^{*2} + \frac{1}{2}m_\omega^2\omega_0^2 + \frac{1}{2}m_\phi^2\phi_0^2 + \frac{1}{2}m_\rho^2\rho_{03}^2 \\ & + \sum_{B=n,p} \frac{2J_B + 1}{2\pi^2} \int_0^{k_{FB}} (k^2 + m_B^{*K^2})^{1/2} k^2 dk + \sum_{l=e^-, \mu^-} \frac{1}{\pi^2} \int_0^{K_{Fl}} (k^2 + m_l^2)^{1/2} k^2 dk \\ & + m_K^* n_{K^-} . \end{aligned} \quad (23)$$

The last term denotes the contribution of the K^- condensate. The pressure in this phase is

$$\begin{aligned} P^K = & -\frac{1}{2}m_\sigma^2\sigma^2 - \frac{1}{3}g_2\sigma^3 - \frac{1}{4}g_3\sigma^4 - \frac{1}{2}m_{\sigma^*}^2\sigma^{*2} + \frac{1}{2}m_\omega^2\omega_0^2 + \frac{1}{2}m_\phi^2\phi_0^2 + \frac{1}{2}m_\rho^2\rho_{03}^2 \\ & + \frac{1}{3} \sum_{B=n,p} \frac{2J_B + 1}{2\pi^2} \int_0^{k_{FB}} \frac{k^4 dk}{(k^2 + m_B^{*K^2})^{1/2}} + \frac{1}{3} \sum_{l=e^-, \mu^-} \frac{1}{\pi^2} \int_0^{K_{Fl}} \frac{k^4 dk}{(k^2 + m_l^2)^{1/2}} . \end{aligned} \quad (24)$$

The mixed phase of hadronic and K^- condensed matter is governed by the Gibbs conditions for thermodynamic equilibrium along with global charge and baryon number conservation laws [35, 45]. The Gibbs phase rules read,

$$P^h = P^K, \quad (25)$$

$$\mu_B^h = \mu_B^K, \quad (26)$$

where μ_B^h and μ_B^K are chemical potentials of baryons B in the pure hadronic and K^- condensed phase, respectively. The global charge neutrality and baryon number conservation laws are

$$(1 - \chi)Q^h + \chi Q^K = 0, \quad (27)$$

$$n_B = (1 - \chi)n_B^h + \chi n_B^K, \quad (28)$$

where χ is the volume fraction of K^- condensed phase in the mixed phase. The total energy density in the mixed phase is given by

$$\epsilon = (1 - \chi)\epsilon^h + \chi\epsilon^K. \quad (29)$$

Pressure and density variations associated with the r-mode oscillation drive the system out of chemical equilibrium. Microscopic reaction processes restore the equilibrium. Weak interaction processes are most important in this situation. The corresponding bulk viscosity coefficient could play a significant role on the mode. Earlier it was shown by various authors [10, 11, 12, 15] that non-leptonic processes involving hyperons might lead to a high value for the bulk viscosity coefficient. The real part of bulk viscosity coefficient is calculated in terms of relaxation times of microscopic processes [12, 46]

$$\zeta = \frac{P(\gamma_\infty - \gamma_0)\tau}{1 + (\omega\tau)^2}, \quad (30)$$

where P is the pressure, τ is the net microscopic relaxation time and γ_∞ and γ_0 are 'infinite' and 'zero' frequency adiabatic indices respectively. The factor

$$\gamma_\infty - \gamma_0 = -\frac{n_b^2}{P} \frac{\partial P}{\partial n_n} \frac{d\bar{x}_n}{dn_b}, \quad (31)$$

can be determined from the equation of state (EoS). Here $\bar{x}_n = \frac{n_n}{n_b}$ gives the neutron fraction in the equilibrium state and $n_b = \sum_B n_B$ is the total baryon density. In the co-rotating frame, the angular velocity (ω) of (l,m) r-mode is related to angular velocity (Ω) of a rotating neutron star as $\omega = \frac{2m}{l(l+1)}\Omega$ [4].

The partial derivatives in both phases are calculated using the Gibbs-Duhem relation. In the pure hadronic phase, this relation gives $P^h = n_n^h \mu_n^h + n_p^h \mu_p^h + n_e \mu_e + n_\mu \mu_e - \epsilon^h$. So the partial derivative is given by

$$\frac{\partial P^h}{\partial n_n^h} = \mu_n^h + n_n^h \frac{\partial \mu_n^h}{\partial n_n^h} + n_p^h \frac{\partial \mu_p^h}{\partial n_n^h} - \frac{\partial \epsilon^h}{\partial n_n^h}. \quad (32)$$

Using $\mu_n^h = \frac{\partial \epsilon^h}{\partial n_n^h}$, we obtain

$$\frac{\partial P^h}{\partial n_n^h} = n_n^h \alpha_{nn}^h + n_p^h \alpha_{pn}^h, \quad (33)$$

where α_{ij} is defined by $\alpha_{ij} = \left(\frac{\partial \mu_i}{\partial n_j} \right)_{n_k, k \neq j}$. Similarly, in the pure condensed phase, the partial derivative is

$$\frac{\partial P^K}{\partial n_n^K} = n_n^K \alpha_{nn}^K + n_p^K \alpha_{pn}^K + n_{K^-} \alpha_{K^-n}^K. \quad (34)$$

In the mixed phase, we obtain the relation

$$\frac{\partial P}{\partial n_n} = \frac{\partial P^h}{\partial n_n^h} + \frac{\partial P^K}{\partial n_n^K} , \quad (35)$$

where $n_n = (1 - \chi)n_n^h + \chi n_n^K$.

We are interested to study the bulk viscosity coefficient and corresponding damping timescale due to the non-leptonic weak decay process (21). For the reaction rate of this process, we may express all perturbed quantities in terms of the variation in neutron number density (n_n^K) in the Bose-Einstein condensed phase. The relaxation time (τ) for the process is given by [12]

$$\frac{1}{\tau} = \frac{\Gamma_K}{\delta\mu} \frac{\delta\mu}{\delta n_n^K} . \quad (36)$$

Here, $\delta n_n^K = n_n^K - \bar{n}_n^K$ is the departure of neutron fraction from its thermodynamic equilibrium value \bar{n}_n^K in the K^- condensed phase. The reaction rate per unit volume can be written as

$$\Gamma_K = \frac{(2\pi)^4}{8(2\pi)^9} \int \frac{d^3k_1}{E_1} \frac{d^3k_2}{E_2} \frac{d^3k_3}{E_3} \langle |\mathcal{M}|^2 \rangle \delta^3(\vec{k}_1 - \vec{k}_2 - \vec{k}_3) F(E_i) \delta^0(E_1 - E_2 - E_3) . \quad (37)$$

where indices $i = 1 - 3$ refer to n , p and K^- respectively. Here we are considering K^- mesons in the s -wave ($\vec{k}_3 = 0$) condensate. So the conservation of momentum gives $\vec{k}_1 = \vec{k}_2$. Assuming that the matrix element has no angular dependence and performing the integrating over d^3k_3 , we get

$$\Gamma_K = \frac{1}{8(2\pi)^5 E_3} \int \frac{|\vec{k}_1| E_1 dE_1}{E_1} \frac{|\vec{k}_2| E_2 dE_2}{E_2} \langle |\mathcal{M}|^2 \rangle F(E_i) \delta^0(E_1 - E_2 - E_3) d\Omega_1 d\Omega_2 , \quad (38)$$

where $F(E_i)$ is the Pauli blocking factor given by

$$F(E_i) = f_1(1 - f_2) - (1 - f_1)f_2 , \quad (39)$$

and $f_i = \frac{1}{(1 + e^{\frac{E_i - \mu_i}{kT}})}$. $|\mathcal{M}|^2$ is the squared matrix element and $\langle . \rangle$ denotes the averaging over initial spins and sum over final spins. In this calculation fermions which reside close to their Fermi surfaces, contribute to the reaction. Integrating over E_1 and substituting $\frac{E_2 - \mu_2}{kT} = y$ and $dE_2 = kT dy$, we obtain

$$\Gamma_K = \frac{\langle |\mathcal{M}|^2 \rangle}{16\pi^3 E_3} k_{F_n}^2 \left(\frac{\delta\mu}{kT} \right) kT \int_{-\infty}^{+\infty} \frac{dy}{(1 + e^{-y})(1 + e^y)} . \quad (40)$$

Finally we arrive at the result,

$$\Gamma_K = \left[\frac{\langle |\mathcal{M}|^2 \rangle}{16\pi^3 E_3} k_{F_n}^2 \right] \delta\mu . \quad (41)$$

Here the in-medium energy of K^- mesons in the condensate is $E_3 = \mu_3 = \mu_{K^-}$ and k_{F_n} is the Fermi momentum for neutrons in the condensed phase. It is noted that the reaction rate per unit volume is proportional to the overall chemical potential imbalance $\delta\mu = \delta\mu_n^K - \delta\mu_p^K - \delta\mu_{K^-}$. Now the relaxation time (36) can be written as

$$\frac{1}{\tau} = \left[\frac{\langle |\mathcal{M}|^2 \rangle}{16\pi^3 \mu_{K^-}} k_{F_n}^2 \right] \frac{\delta\mu}{\delta n_n^K} . \quad (42)$$

Next we focus on the evaluation of the matrix element of the non-leptonic process (21). In the general form, this can be written as [47, 48]

$$\mathcal{M} = \bar{u}(k_2) (A + B\gamma_5) u(k_1) , \quad (43)$$

where $u(k_1)$ and $u(k_2)$ are the spinors of neutrons and protons respectively. Here A is the parity violating amplitude and B is the parity conserving amplitude. The squared matrix element is given by

$$\langle |\mathcal{M}|^2 \rangle = 2[(k_1 \cdot k_2 + m_n^{*K} m_p^{*K}) |A|^2 + (k_1 \cdot k_2 - m_n^{*K} m_p^{*K}) |B|^2] . \quad (44)$$

As fermion momenta lie close to their Fermi surfaces, we can write $k_1 \cdot k_2 = E_1 E_2 - |\vec{k}_1| |\vec{k}_2| \cos \theta = \mu_n^K \mu_p^K - k_{F_n}^2$. This leads to the squared matrix element

$$\langle |\mathcal{M}|^2 \rangle = 2[(\mu_n^K \mu_p^K - k_{F_n} k_{F_p} + m_n^{*K} m_p^{*K}) |A|^2 + (\mu_n^K \mu_p^K - k_{F_n} k_{F_p} - m_n^{*K} m_p^{*K}) |B|^2] . \quad (45)$$

Here we apply the weak SU(3) symmetry to the non-leptonic weak decay amplitudes for the process (21). Earlier weak decays of the octet hyperons were described by an effective SU(3) interaction with a parity violating (A) and parity conserving (B) amplitudes [49, 50]. The weak operator is proportional to Gell-Mann matrix λ_6 to ensure hypercharge violation $|\Delta Y| = 1$ and $|\Delta I| = 1/2$ rule. The amplitudes were determined experimentally from the weak decay parameters of the octet hyperons [50]. We follow the same mechanism to determine the amplitudes in (21). The amplitudes are $A = -1.62 \times 10^{-7}$ and $B = -7.1 \times 10^{-7}$.

The computation of the relaxation time is complete with the calculation of $\frac{\delta\mu}{\delta n_n^K}$. The chemical potential imbalance due to the non-leptonic process (21) is given by

$$\begin{aligned} \delta\mu &= \delta\mu_n^K - \delta\mu_p^K - \delta\mu_{K^-} \\ &= (\alpha_{nn}^K \delta n_n^K + \alpha_{np}^K \delta n_p^K + \alpha_{nK^-} \delta n_{K^-}) \\ &\quad - (\alpha_{pn}^K \delta n_n^K + \alpha_{pp}^K \delta n_p^K + \alpha_{pK^-} \delta n_{K^-}) \\ &\quad - (\alpha_{K^-n} \delta n_n^K + \alpha_{K^-p} \delta n_p^K + \alpha_{K^-K^-} \delta n_{K^-}) . \end{aligned} \quad (46)$$

We express $\delta\mu$ in terms of δn_n^K and obtain $\frac{\delta\mu}{\delta n_n^K}$ from the following constraints,

$$\begin{aligned}
(1 - \chi)(\delta n_n^h + \delta n_p^h) + \chi(\delta n_n^K + \delta n_p^K) &= 0, \\
(1 - \chi)\delta n_p^h + \chi(\delta n_p^K - \delta n_{K^-}) &= 0, \\
\delta\mu_p^h &= \delta\mu_p^K, \\
\delta\mu_n^h &= \delta\mu_n^K.
\end{aligned} \tag{47}$$

In the above constraints, we have $\delta\chi = 0$ because number densities deviate from their equilibrium values not by changing the volume of the fluid element but by internal reactions [12]. First two constraints result from the conservation of baryon number and electric charge neutrality. The other constraints are due to the equality of neutron and proton chemical potentials in the hadronic and condensed phases. Further the last two constraints in (47) can be written as

$$\begin{aligned}
(\alpha_{pn}^h \delta n_n^h + \alpha_{pp}^h \delta n_p^h) - (\alpha_{pn}^K \delta n_n^K + \alpha_{pp}^K \delta n_p^K + \alpha_{pK^-} \delta n_{K^-}) &= 0, \\
(\alpha_{nn}^h \delta n_n^h + \alpha_{np}^h \delta n_p^h) - (\alpha_{nn}^K \delta n_n^K + \alpha_{np}^K \delta n_p^K + \alpha_{nK^-} \delta n_{K^-}) &= 0.
\end{aligned} \tag{48}$$

Next we calculate α_{ij} in the hadronic as well as K^- condensed phases using the EoS. These quantities in the hadronic phase are given by

$$\begin{aligned}
\alpha_{nn}^h &= \frac{\partial\mu_n^h}{\partial n_n^h} \\
&= \left(\frac{g_{\omega N}}{m_\omega}\right)^2 + \frac{1}{4} \left(\frac{g_{\rho N}}{m_\rho}\right)^2 + \frac{\pi^2}{k_{F_n} \sqrt{k_{F_n}^2 + m_N^{*h2}}} - \frac{m_N^{*h} g_{\sigma N}}{\sqrt{k_{F_n}^2 + m_N^{*h2}}} \frac{\partial\sigma}{\partial n_n^h},
\end{aligned} \tag{49}$$

$$\alpha_{np}^h = \left(\frac{g_{\omega N}}{m_\omega}\right)^2 - \frac{1}{4} \left(\frac{g_{\rho N}}{m_\rho}\right)^2 - \frac{m_N^{*h} g_{\sigma N}}{\sqrt{k_{F_n}^2 + m_N^{*h2}}} \frac{\partial\sigma}{\partial n_p^h}, \tag{50}$$

where

$$\frac{\partial\sigma}{\partial n_n^h} = \frac{\left(\frac{g_{\sigma N}}{m_\sigma^2}\right) \frac{m_N^{*h}}{\sqrt{k_{F_n}^2 + m_N^{*h2}}}}{D}, \tag{51}$$

$$\frac{\partial\sigma}{\partial n_p^h} = \frac{\left(\frac{g_{\sigma N}}{m_\sigma^2}\right) \frac{m_N^{*h}}{\sqrt{k_{F_p}^2 + m_N^{*h2}}}}{D}, \tag{52}$$

and

$$D = 1 + \frac{1}{m_\sigma^2} \frac{d^2 U}{d\sigma^2} + \sum_{B=n,p} \frac{(2J_B + 1)}{2\pi^2} \left(\frac{g_{\sigma B}}{m_\sigma}\right)^2 \int_0^{K_{FB}} \frac{k^4 dk}{(k^2 + m_B^{*h2})^{3/2}}. \tag{53}$$

Also, α_{pp}^h and α_{pn}^h are obtained by interchanging $n \leftrightarrow p$ in α_{nn}^h and α_{np}^h respectively. Similarly, α_{ij} in the K^- condensed phase are given by

$$\alpha_{nn}^K = \frac{\partial \mu_n^K}{\partial n_n^K} = \left(\frac{g_{\omega N}}{m_\omega} \right)^2 + \frac{1}{4} \left(\frac{g_{\rho N}}{m_\rho} \right)^2 + \frac{\pi^2}{k_{F_n} \sqrt{k_{F_n}^2 + m_N^{*K^2}}} - \frac{m_N^{*K} g_{\sigma N}}{\sqrt{k_{F_n}^2 + m_N^{*K^2}}} \frac{\partial \sigma}{\partial n_n^K}, \quad (54)$$

$$\alpha_{np}^K = \left(\frac{g_{\omega N}}{m_\omega} \right)^2 - \frac{1}{4} \left(\frac{g_{\rho N}}{m_\rho} \right)^2 - \frac{m_N^{*K} g_{\sigma N}}{\sqrt{k_{F_n}^2 + m_N^{*K^2}}} \frac{\partial \sigma}{\partial n_p^K}, \quad (55)$$

$$\alpha_{nK^-} = \frac{\partial \mu_n^K}{\partial n_{K^-}} = - \left(\frac{g_{\omega N} g_{\omega K}}{m_\omega^2} \right) + \frac{1}{4} \left(\frac{g_{\rho N} g_{\rho K}}{m_\rho^2} \right) - \frac{m_N^{*K} g_{\sigma N}}{\sqrt{k_{F_n}^2 + m_N^{*K^2}}} \frac{\partial \sigma}{\partial n_{K^-}}, \quad (56)$$

$$\alpha_{K^-n} = \frac{\partial \mu_{K^-}}{\partial n_n^K} = - \left(\frac{g_{\omega N} g_{\omega K}}{m_\omega^2} \right) + \frac{1}{4} \left(\frac{g_{\rho N} g_{\rho K}}{m_\rho^2} \right) - g_{\sigma K} \frac{\partial \sigma}{\partial n_n^K}, \quad (57)$$

$$\alpha_{K^-K^-} = \frac{\partial \mu_{K^-}}{\partial n_{K^-}} = \left(\frac{g_{\omega K}}{m_\omega} \right)^2 + \left(\frac{g_{\phi K}}{m_\phi} \right)^2 + \frac{1}{4} \left(\frac{g_{\rho K}}{m_\rho} \right)^2 - g_{\sigma K} \frac{\partial \sigma}{\partial n_{K^-}} - g_{\sigma^* K} \frac{\partial \sigma^*}{\partial n_{K^-}}, \quad (58)$$

where,

$$\begin{aligned} \frac{\partial \sigma}{\partial n_n^K} &= \left(\frac{g_{\sigma N}}{m_\sigma^2} \right) \frac{\frac{m_N^{*K}}{\sqrt{k_{F_n}^2 + m_N^{*K^2}}}}{D'}, \\ \frac{\partial \sigma}{\partial n_{K^-}} &= \frac{\frac{g_{\sigma K}}{m_\sigma^2}}{D'}, \\ \frac{\partial \sigma^*}{\partial n_{K^-}} &= \frac{\frac{g_{\sigma^* K}}{m_{\sigma^*}^2}}{D'}, \end{aligned} \quad (59)$$

and $\frac{\partial \sigma^*}{\partial n_n^K} = \frac{\partial \sigma^*}{\partial n_p^K} = 0$. Here D' has the same form as D in (53), but D' has to be calculated using the meson fields in the condensed phase. The coefficients α_{pp}^K , α_{pn}^K , α_{pK^-} and α_{K^-p} are obtained by interchanging $n \leftrightarrow p$ in α_{nn}^K , α_{np}^h , α_{nK^-} and α_{K^-n} respectively.

The bulk viscosity damping timescale (τ_B) due to the non-leptonic process (21) is defined by

$$\frac{1}{\tau_B} = - \frac{1}{2E} \frac{dE}{dt}, \quad (60)$$

where E is the energy of the perturbation in the co-rotating frame of the fluid and is given by [12]

$$E = \frac{1}{2} \alpha^2 \Omega^2 R^{-2} \int_0^R \epsilon(r) r^6 dr. \quad (61)$$

Here α is the dimensionless amplitude of the r-mode, R is the radius of the star and $\epsilon(r)$ is the energy density profile. The rate of energy dissipation is given by

$$\frac{dE}{dt} = -4\pi \int_0^R \zeta(r) < |\vec{\nabla} \cdot \delta \vec{v}|^2 > r^2 dr, \quad (62)$$

where the angle average of the square of the hydrodynamic expansion [15, 51] is $\langle |\vec{\nabla} \cdot \delta \vec{v}|^2 \rangle = \frac{(\alpha\Omega)^2}{690} \left(\frac{r}{R}\right)^6 \left[1 + 0.86 \left(\frac{r}{R}\right)^2\right] \left(\frac{\Omega^2}{\pi G \bar{\epsilon}}\right)^2$ and $\bar{\epsilon}$ is the mean energy density of a non-rotating star. Equation (60) is the bulk viscosity contribution to the imaginary part of the r-mode frequency. We also take into account time scales associated with gravitational radiation (τ_{GR}), bulk viscosity due to modified Urca process (τ_U) involving only nucleons and the shear viscosity (τ_{SV}) and define the overall r-mode time scale (τ_r) as

$$\frac{1}{\tau_r} = -\frac{1}{\tau_{GR}} + \frac{1}{\tau_B} + \frac{1}{\tau_U} + \frac{1}{\tau_{SV}} . \quad (63)$$

The gravitational radiation timescale is given by [7]

$$\frac{1}{\tau_{GR}} = \frac{131072\pi}{164025} \Omega^6 \int_0^R \epsilon(r) r^6 dr . \quad (64)$$

The time scale corresponding to the bulk viscosity due to the modified Urca process (τ_U) involving only nucleons is calculated in the same footing as the bulk viscosity damping time scale due to the non-leptonic process but using the following expression for the bulk viscosity coefficient for the modified Urca process given by [3, 52]

$$\zeta_U = 6 \times 10^{25} \left(\frac{\epsilon}{10^{15} g/cm^3}\right)^2 \left(\frac{T}{10^9 K}\right)^6 \left(\frac{\omega}{1 Hz}\right)^{-2} g/cms . \quad (65)$$

The damping time scale due to the shear viscosity is given by [7]

$$\frac{1}{\tau_{SV}} = 5 \int_0^R \eta(r) r^4 dr \left(\int_0^R \epsilon(r) r^6 dr\right)^{-1} . \quad (66)$$

Different scattering processes contribute to the shear viscosity (η) depending on whether neutrons and protons are superfluid or not [3, 18]. In this calculation, neutrons and protons are both normal fluids. The most important contribution comes from neutron-neutron scattering in this case and the shear viscosity coefficient has the form [3],

$$\eta = 2 \times 10^{18} \left(\frac{\epsilon}{10^{15} g/cm^3}\right)^{9/4} \left(\frac{T}{10^9 K}\right)^{-2} g/cms . \quad (67)$$

The total r-mode time scale is a function of angular velocity, neutron star mass and temperature. Therefore, solving $\frac{1}{\tau_r} = 0$, we calculate the critical angular velocity above which the r-mode is unstable whereas it is stable below the critical angular velocity.

III. RESULTS AND DISCUSSION

We need to know meson-nucleon and meson-kaon coupling constants for this calculation. The nucleon-meson coupling constants are determined from the nuclear matter saturation properties of binding energy $E/B = -16.3$ MeV, baryon density $n_0 = 0.153 \text{ fm}^{-3}$, asymmetry energy coefficient $a_{\text{asy}} = 32.5$ MeV, incompressibility $K = 240$ MeV and effective nucleon mass $m_N^*/m_N = 0.70$. The coupling constants are taken from Ref.[53] and this set is known as GM. We determine kaon-meson coupling constants using the quark model and isospin counting rule. The vector coupling constants are given by

$$g_{\omega K} = \frac{1}{3}g_{\omega N} \quad \text{and} \quad g_{\rho K} = g_{\rho N} . \quad (68)$$

The scalar coupling constant is obtained from the real part of K^- optical potential depth at normal nuclear matter density

$$U_{\bar{K}}(n_0) = -g_{\sigma K}\sigma - g_{\omega K}\omega_0 . \quad (69)$$

It was found in various calculations that antikaons experienced an attractive potential and kaons had a repulsive interaction in nuclear matter [54, 55, 56, 57, 58, 59]. The strength of antikaon optical potential ranges from shallow (-40 MeV) to strongly attractive (-180 MeV). Moreover, it was noted that K^- condensation could be a possibility for antikaon potential ~ 100 MeV or more attractive. Here we perform the calculation for a set of values of antikaon optical potential depths at normal nuclear matter density. We obtain kaon-scalar meson coupling constants $g_{\sigma K} = 2.1914, 3.0426, 3.8937$ corresponding to $U_{\bar{K}}(n_0) = -100, -120, -140$ MeV.

The strange meson fields couple with (anti)kaons. The σ^* -K coupling constant is $g_{\sigma^* K} = 2.65$ as determined from the decay of $f_0(925)$ and the vector ϕ meson coupling with (anti)kaons $\sqrt{2}g_{\phi K} = 6.04$ follows from the SU(3) relation [38].

We begin our investigation with K^- condensation in nuclear matter and denote this system as $\text{np}K^-$. Baryon densities corresponding to lower ($u_l = n_l/n_0$) and upper ($u_u = n_u/n_0$) boundaries for K^- condensation with antikaon optical potential depths at normal nuclear matter density $U_{\bar{K}}(n_0) = -100, -120, -140$ MeV are shown in Table I. The K^- condensation sets in at a density $n_l = u_l n_0$ and a pure K^- condensed phase with nucleons embedded in it begins at a density $n_u = u_u n_0$. It is evident from the Table that there is no mixed

phase for $U_{\bar{K}}(n_0) = -100$ MeV. We further note that the phase transition is of second order for $|U_{\bar{K}}(n_0)| \leq 100$ MeV. On the other hand, the onset of K^- condensation shifts towards lower density as the antikaon optical potential becomes more attractive. The mixed phase is found to be wider for $U_{\bar{K}}(n_0) = -140$ MeV. These findings were already reported in Ref. [35]. Another interesting problem arises when hyperons appear around threshold densities of K^- condensation. We showed in an earlier calculation [16] by extending the Lagrangian density in (1) to include hyperons that Λ hyperons first appeared around baryon density $2.58n_0$. However, Σ hyperons are excluded from the system because of a strongly repulsive Σ -nuclear matter interaction whereas massive Ξ hyperons appear at higher densities. In this context, we continue our calculation with K^- condensation in np Λ matter denoted by np ΛK^- . In this case, Λ -meson couplings are taken from Ref.[16]. The threshold density (u_{th}^Λ) for the appearance of Λ hyperons are listed in Table I. For $U_{\bar{K}}(n_0) = -100, -120$ MeV, Λ hyperons appear before the K^- condensate. Consequently, K^- condensation is delayed to higher densities. Those values are recorded in parentheses. On the other hand, the early occurrence of K^- condensation for $U_{\bar{K}}(n_0) = -140$ MeV delays the appearance of Λ hyperons to higher density. Therefore, the composition of matter and the strength of antikaon optical potential depth determine the onset of K^- condensate and Λ hyperons in np ΛK^- matter. It was already noted that the bulk viscosity coefficient due to the non-leptonic process involving Λ hyperons had a very large value. In this calculation, we study the bulk viscosity due to non-leptonic process (21) in np K^- matter and find out whether kaon bulk viscosity alone can damp the r-mode without hyperons.

Now we describe the composition of β -equilibrated and charge neutral matter in the presence of K^- condensation for $U_{\bar{K}}(n_0) = -120$ MeV. Populations of various particles are displayed in Fig. 1. Before the appearance of K^- condensate, particle fractions increase with baryon density. In this situation, charge neutrality is maintained among protons, electrons and muons. The mixed phase begins with the onset of K^- condensation at $3.26 n_0$. As soon as K^- condensate is formed, its rapid growth replaces electrons and muons from the system. Consequently, the proton density becomes equal to the density of K^- mesons in the condensate.

The equations of state, pressure versus energy density, with and without K^- condensate are shown in Fig. 2. The solid line represents the overall EoS without K^- condensate whereas the long dashed, short dashed and dotted lines correspond to those with the conden-

sate for $U_{\bar{K}} = -100, -120, -140$ MeV respectively. We have already noted that the phase transition is of second order for $U_{\bar{K}}(n_0) = -100$ MeV. On the other hand, we find that two kinks on the EoS involving the condensate mark the beginning and end of the mixed phase for $U_{\bar{K}}(n_0) = -120, -140$ MeV. The EoS becomes softer in the presence of K^- condensate compared with the case without the condensate. The deeper the antikaon optical potential depth, the softer is the EoS.

Next we construct models of non-rotating and uniformly rotating neutron stars [60] using EoS as shown in Fig. 2. The gravitational mass for non-rotating neutron star sequence and the sequence of neutron stars rotating at their Kepler frequencies are plotted with central energy density ϵ_c in Fig. 3. The inclusion of K^- condensate in EoS for different values of $U_{\bar{K}}(n_0)$ reduces maximum masses for non-rotating as well as rotating neutron stars. The maximum gravitational masses, equatorial radii, corresponding central baryon and energy densities and Kepler periods for the mass shedding limit are given by Table II. The corresponding values for non-rotating neutron stars are shown in parentheses. It is evident from Table II that the softest EoS corresponding to $U_{\bar{K}}(n_0) = -140$ MeV leads to a maximum non-rotating neutron star mass $1.343 M_\odot$ which is well below the most accurately measured Hulse-Taylor pulsar mass $1.44 M_\odot$. Therefore, this EoS is ruled out by observations. We adopt antikaon optical potential depths $U_{\bar{K}}(n_0) = -100, -120$ MeV for the calculation of bulk viscosity.

The equation of state enters as an input in the calculations of adiabatic indices, relaxation time and bulk viscosity coefficient. In particular, partial derivatives of pressure and chemical potentials with respect to neutron number density are calculated using the EoS. Figure 4 exhibits the difference of fast and slow adiabatic indices as a function of normalised baryon density for $U_{\bar{K}}(n_0) = -100, -120$ MeV. We find jumps in the difference of adiabatic indices $(\gamma_\infty - \gamma_0)$. For $U_{\bar{K}}(n_0) = -100$ MeV, this jump occurs at the onset of K^- condensation whereas these are attributed to kinks on the EoS for $U_{\bar{K}} = -120$ MeV in Fig. 2. Those kinks lead to discontinuities in the partial derivatives in Eq. (31). This kind of jump in adiabatic indices was earlier noted in quark-hadron phase transition in neutron star matter by others [61]. We further note that the value of $(\gamma_\infty - \gamma_0)$ is suppressed for $U_{\bar{K}}(n_0) = -100$ MeV compared with the case of $U_{\bar{K}}(n_0) = -120$ MeV. The relaxation time for the non-leptonic weak process (21) is plotted with normalised baryon density in Fig. 5 for different values of antikaon optical potential depths. In this case, the maximum value of relaxation time

is $\sim 10^{-11}s$ for $U_{\bar{K}}(n_0) = -120$ MeV. This value is a few order of magnitude smaller than that of the non-leptonic process involving non-superfluid Λ hyperons [15, 16]. Also, we note that the relaxation time given by Eq. (42) is independent of temperature because there is no temperature dependence in the reaction rate in (41). This may be attributed to the fact that the K^- condensate is treated here as a zero temperature Bose-Einstein condensate. On the other hand, the relaxation time for the non-leptonic weak process involving hyperons was found to be inversely proportional to T^2 [12, 15, 16]. It is worth mentioning here that the role of thermal kaon processes in the non-equilibrium dynamics of kaon condensation was studied by others [62, 63].

The bulk viscosity coefficient in the kaon condensed phase is shown as a function of normalised baryon density in Fig. 6. The factor $\omega\tau$ in the bulk viscosity coefficient given by Eq. (30) is negligible compared with unity over the whole range of baryon densities considered here. We note that the bulk viscosity coefficient is discontinuous at the phase boundaries of hadronic and K^- condensed matter. This is attributed to kinks in the EoS and discontinuities in $(\gamma_\infty - \gamma_0)$. It is worth mentioning here that the bulk viscosity coefficient in the kaon condensed matter is several orders of magnitude smaller than the non-superfluid hyperon bulk viscosity coefficient [12, 15, 16]. We also note that the bulk viscosity coefficient is larger for $U_{\bar{K}}(n_0) = -120$ MeV than that of the case with $U_{\bar{K}}(n_0) = -100$ MeV in the lower density regime. We use the bulk viscosity coefficient corresponding to $U_{\bar{K}}(n_0) = -120$ MeV for the calculation of damping time scale and critical angular velocity.

The computation of damping time scale due to bulk viscosity given by Eq. (60) involves the energy density profile, kaon bulk viscosity profile and structures of rotating neutron stars. The sequence of neutron stars rotating at Kepler frequencies is calculated by using the model of Stergioulas [60]. We have already shown the mass shedding limit sequences of rotating neutron stars in Fig. 3. For the calculation of damping time scale, rotating neutron stars which contain K^- condensate in its interior are to be considered. The appearance of K^- condensate is sensitive to the central density of a rotating neutron star which, in turn, depends on the rotation period of the star. It is worth mentioning here that the canonical neutron star of $1.4M_\odot$ rotating at the Kepler period 1.22 ms has a central baryon density $2.20n_0$ and that of its non-rotating counterpart has a central baryon density $2.76n_0$ for $U_{\bar{K}}(n_0) = -100, -120$ MeV. This shows that central densities of $1.4M_\odot$ canonical neutron star are well below threshold densities of K^- condensation. To demonstrate the effect of

kaon bulk viscosity on the r-mode instability, we choose a neutron star of gravitational mass $1.63M_{\odot}$ having central baryon density $3.94 n_0$ and rotating at an angular velocity $\Omega_{rot} = 1180s^{-1}$ from the sequence of rotating neutron stars corresponding to $U_{\bar{K}} = -120$ MeV. This neutron star contains K^{-} condensate in its core because the central baryon density is well above the threshold density of K^{-} condensation. The energy density profile of this rotating star is plotted as a function of equatorial distance in Fig. 7. Similarly, the kaon bulk viscosity profile of this neutron star as a function of equatorial distance is shown in Fig. 8. Here we note that the bulk viscosity profile drops to zero value beyond 2 km. This happens because the baryon density beyond 2 km decreases below the threshold density of K^{-} condensation and the non-leptonic process (21) ceases to occur there.

Using the energy density and bulk viscosity profiles, we estimate the damping time scale corresponding to the bulk viscosity due to the non-leptonic process (21). We also consider the contributions of modified Urca process involving nucleons as well as the shear viscosity to the total r-mode time scale as given by Eq. (63). We obtain critical angular velocities as a function of temperature solving $1/\tau_r = 0$ for a rotating neutron star mass $1.63M_{\odot}$ corresponding to the case $U_{\bar{K}}(n_0) = -120$ MeV and show this in Fig. 9. The r-mode is unstable above the critical angular velocity curve and stable below it. The bulk viscosity due to the modified Urca process dominates at higher temperatures and might damp the r-mode instability. The long dashed line which merges with the solid line above 5×10^9 K, shows the modified Urca contribution balancing the gravitational radiation reaction. As temperature decreases, the bulk viscosity due to the modified Urca process also decreases. Consequently the corresponding damping time scale due to the modified Urca process is longer than the gravitational radiation growth time scale and the r-mode instability is not suppressed below 10^9 K by this process. Now we consider the shear viscosity. As the shear viscosity coefficient is proportional to T^{-2} , it might suppress the instability at lower temperatures. This is shown by the short dashed line which merges with the solid line below temperature 5×10^9 K. Next we discuss what is the influence of kaon bulk viscosity on the r-mode instability. We know already that kaon bulk viscosity is independent of temperature. The bulk viscosity damping time scale (τ_B) due to the non-leptonic process (21) and the time scale associated with gravitational radiation are also independent of temperature but depend on angular velocity (Ω). Further investigation reveals that the damping time scale τ_B is always longer than the gravitational radiation growth time scale τ_{GR} for all values of Ω ranging from 0 to Ω_{rot} . This

implies that the bulk viscosity due to the non-leptonic process in K^- condensed matter can not damp the r-mode instability. When all viscous processes are taken into account, we find an intermediate temperature regime where neither shear viscosity nor bulk viscosity can damp the r-mode instability, is marked by the solid line. The critical angular velocity curve is determined due to the interplay of τ_U , τ_{SV} and τ_{GR} .

IV. SUMMARY AND CONCLUSIONS

We have investigated the role of K^- condensation on bulk viscosity and r-mode instability in neutron stars. The bulk viscosity coefficient and the corresponding damping time scale due to the non-leptonic process $n \rightleftharpoons p + K^-$ have been calculated. In this calculation, we have considered first and second order kaon condensation and constructed equations of state for different values of antikaon optical potential depths within the framework of relativistic field theoretical models. It is noted that kaon bulk viscosity and the corresponding damping time scale are independent of temperature. We find that the bulk viscosity coefficient in K^- condensed matter is suppressed by several orders of magnitude compared with the non-superfluid hyperon bulk viscosity coefficient[12, 15, 16]. Further we note that kaon bulk viscosity due to the process (21) alone can not damp the r-mode instability because kaon bulk viscosity damping time scale is always longer than the gravitational radiation growth time scale.

We have also discussed the role of hyperons on the appearance of K^- condensate. The early appearance of Λ hyperons delays the onset of K^- condensation to higher densities for antikaon optical potential depths $U_{\bar{K}}(n_0) = -100, -120$ MeV. For $U_{\bar{K}}(n_0) = -140$ MeV, K^- condensation occurs before Λ hyperons are populated in the system. The latter situation was already reported in Ref. [42] for a different parameter set. In this connection, we note that the large value of hyperon bulk viscosity might damp the r-modes in neutron stars when hyperons appear in neutron stars. On the other hand, the r-modes in neutron stars containing only kaon condensate could be damped by the bulk viscosity of modified Urca process at higher temperatures and by the shear viscosity at lower temperatures as it is demonstrated in Fig. 9. It is to be noted here that the onset of K^- condensation is very sensitive to the rotation period of the neutron star under investigation. The gravitational instability window for the case with K^- condensate in nuclear matter would be different

from the situation when hyperons are included with the condensate.

V. ACKNOWLEDGMENTS

We thank Jürgen Schaffner-Bielich for many fruitful discussions. DB thanks the Alexander von Humboldt Foundation for the fellowship. We also thank Horst Stöcker and Walter Greiner for their support and acknowledge the warm hospitality at the Institute for Theoretical Physics, J.W. Goethe University, Frankfurt am Main and Frankfurt Institute for Advanced Studies (FIAS) where a part of this work was completed.

-
- [1] S. Chandrasekhar, Phys. Rev. Lett. **24**, 611 (1970).
 - [2] J. L. Friedman and B. F. Schutz, Astrophys. J. **221**, 937 (1978);
J. L. Friedman and B. F. Schutz, Astrophys. J. **222**, 281 (1978);
J. L. Friedman Commun. Math. Phys. **62**, 247 (1978).
 - [3] N. Andersson and K.D. Kokkotas, Int. J. Mod. Phys. **D10**, 381 (2001).
 - [4] N. Andersson, Class. Quant. Grav. **20**, R105 (2003).
 - [5] N. Andersson, Astrophys J. **502**, 708 (1998).
 - [6] J. L. Friedman and S. M. Morsink, Astrophys J. **502**, 714 (1998).
 - [7] L. Lindblom, B.J. Owen and S. M. Morsink, Phys. Rev. Lett. **80**, 4843 (1998).
 - [8] N. Andersson, K. D. Kokkotas and B. F. Schutz, Astrophys J. **510**, 846 (1999).
 - [9] N. Stergioulas, Liv. Rev. Rel. **6**, 3 (2003).
 - [10] P.B. Jones, Phys. Rev. Lett. **86**, 1384 (2001).
 - [11] P.B. Jones, Phys. Rev. D **64**, 084003 (2001).
 - [12] L. Lindblom and B.J. Owen, Phys. Rev. D **65**, 063006 (2002).
 - [13] E.N.E. van Dalen and A.E.L. Dieperink, Phys. Rev. C **69**, 025802 (2004).
 - [14] A. Drago, A. Lavagno and G. Pagliara, Phys. Rev. D **71**, 103004 (2005).
 - [15] M. Nayyar and B.J. Owen, Phys. Rev. D **73**, 084001 (2006).
 - [16] D. Chatterjee and D. Bandyopadhyay, Phys. Rev. D **74**, 023003 (2006);
D. Chatterjee and D. Bandyopadhyay, astro-ph/0607005.
 - [17] Haensel P., Levenfish K.P., Yakovlev D.G. Astron. Astrophys., **357**, 1157 (2000);

- Haensel P., Levenfish K.P., Yakovlev D.G. *Astron. Astrophys.*, **372**, 130 (2001);
 Haensel P., Levenfish K.P., Yakovlev D.G. *Astron. Astrophys.*, **381**, 1080 (2002).
- [18] N. Andersson, *astro-ph/0610192*.
- [19] L. Lindblom and G. Mendell, *Phys. Rev. D* **61**, 104003 (2000).
- [20] J. Madsen, *Phys. Rev. D* **46**, 3290 (1992).
- [21] J. Madsen, *Phys. Rev. Lett.* **85**, 10 (2000).
- [22] H. Dong, N. Su and Q. Wang, *Phys. Rev. D* **75**, 074016 (2007).
- [23] H. Dong, N. Su and Q. Wang, *astro-ph/0702181*.
- [24] N.N. Pan, X.P. Zheng and J.R. Li, *Mon. Not. Roy. Astron. Soc.* **371**, 1359 (2006).
- [25] B.A. Sa'd, I.A. Shovkovy and D.H. Rischke, *Phys. Rev. D* **75**, 065016 (2007).
- [26] M.G. Alford and A. Schmidt, *J. Phys. G* **34**, 67 (2007).
- [27] M.G. Alford, M. Braby, S. Reddy and T. Schafer, *nucl-th/0701067*.
- [28] B.A. Sa'd, I.A. Shovkovy and D.H. Rischke, *astro-ph/0703016*.
- [29] D.B. Kaplan and A.E. Nelson, *Phys. Lett. B* **175**, 57 (1986);
 A.E. Nelson and D.B. Kaplan, *Phys. Lett. B* **192**, 193 (1987).
- [30] G.E. Brown, K. Kubodera, M. Rho and V. Thorsson, *Phys. Lett. B* **291**, 355 (1992).
- [31] V. Thorsson, M. Prakash and J.M. Lattimer, *Nucl. Phys.* **A572**, 693 (1994).
- [32] P.J. Ellis, R. Knorren and M. Prakash, *Phys. Lett. B* **349**, 11 (1995).
- [33] M. Prakash, I. Bombaci, M. Prakash, P.J. Ellis, J.M. Lattimer and R. Knorren, *Phys. Rep.* **280**, 1 (1997).
- [34] N.K. Glendenning and J. Schaffner-Bielich, *Phys. Rev. Lett.* **81**, 4564 (1998).
- [35] N.K. Glendenning and J. Schaffner-Bielich, *Phys. Rev. C* **60**, 025803 (1999).
- [36] T. Muto, *Prog. Theo. Phys.* **89**, 415 (1993).
- [37] R. Knorren, M. Prakash and P.J. Ellis, *Phys. Rev. C* **52**, 3470 (1995).
- [38] J. Schaffner and I.N. Mishustin, *Phys. Rev. C* **53**, 1416 (1996).
- [39] J.A. Pons, S. Reddy, P.J. Ellis, M. Prakash, and J.M. Lattimer, *Phys. Rev. C* **62**, 035803 (2000).
- [40] S. Pal, D. Bandyopadhyay and W. Greiner, *Nucl. Phys.* **A674**, 553 (2000).
- [41] S. Banik and D. Bandyopadhyay, *Phys. Rev. C* **63**, 035802 (2001).
- [42] S. Banik and D. Bandyopadhyay, *Phys. Rev. C* **64**, 055805 (2001).
- [43] J. Boguta and A.R. Bodmer, *Nucl. Phys.* **A292**, 413 (1977).

- [44] B.D. Serot and J.D. Walecka, Adv. in Nucl. Phys. **16**, 1 (1986).
- [45] N.K. Glendenning, Phys. Rev. D **46**, 1274 (1992).
- [46] L.D. Landau and E.M. Lifshitz, Fluid Mechanics, (Butterworth-Heinemann, Oxford, 1999).
- [47] E.D. Commins, Weak Interactions (McGraw-Hill, New York, 1973).
- [48] L.B. Okun, Leptons and Quarks (North-Holland, Amsterdam, 1982).
- [49] R.E. Marshak, Riazuddin and C.P. Ryan, Theory of weak interactions in particle physics (Wiley-Interscience, New York, 1969).
- [50] J. Schaffner-Bielich, R. Mattiello and H. Sorge, Phys. Rev. Lett. **84**, 4305 (2000).
- [51] L. Lindblom, G. Mendell and B.J. Owen, Phys. Rev. D **60**, 064006 (1999).
- [52] R.F. Sawyer, Phys. Rev. D **39**, 3804 (1989).
- [53] N.K. Glendenning and S.A. Moszkowski, Phys. Rev. Lett. **67**, 2414 (1991).
- [54] E. Friedman, A. Gal and C.J. Batty, Nucl. Phys. **A579**, 518 (1994);
C.J. Batty, E. Friedman and A. Gal, Phys. Rep. **287**, 385 (1997).
- [55] E. Friedman, A. Gal, J. Mareš and A. Cieplý, Phys. Rev. C **60**, 024314 (1999).
- [56] V. Koch, Phys. Lett. B **337**, 7 (1994).
- [57] T. Waas and W. Weise, Nucl. Phys. **A625**, 287 (1997).
- [58] G.Q. Li, C.-H. Lee and G.E. Brown, Phys. Rev. Lett. **79**, 5214 (1997); Nucl. Phys. **A625**, 372 (1997).
- [59] S. Pal, C.M. Ko, Z. Lin and B. Zhang, Phys. Rev. C **62**, 061903(R) (2000).
- [60] N. Stergioulas and J. L. Friedman, Astrophys. J. **444**, 306 (1995).
- [61] N.A. Gentile *et al.*, Astrophys. J. **414**, 701 (1993).
- [62] T. Muto, T. Tatsumi and N. Iwamoto, Phys. Rev. **D61**, 063001 (2000).
- [63] T. Muto, T. Tatsumi and N. Iwamoto, Phys. Rev. **D61**, 083002 (2000).

TABLE I: For neutron star matter with nucleons and antikaon condensate (npK^-), baryon densities $u = n/n_0$, corresponding to the lower (u^l) and upper (u^u) boundaries of the mixed phase for first order K^- condensation at various values of antikaon optical potential depths $U_{\bar{K}}(n_0)$ (in MeV) at the saturation density $n_0 = 0.153 \text{ fm}^{-3}$ are given by this table. Threshold densities of Λ hyperons, u_{th}^Λ , are shown for neutron star matter composed of nucleons, Λ hyperons and K^- condensate. The values in parentheses are obtained in the presence of Λ hyperons.

$U_{\bar{K}}(n_0)$	u^l	u^u	u_{th}^Λ
-100	3.88 (4.70)	3.88 (4.70)	2.58
-120	3.26 (3.47)	4.62 (5.35)	2.58
-140	2.46 (2.46)	5.40 (6.07)	3.91

TABLE II: Maximum masses M_{max} , equatorial radii R and their corresponding central baryon densities $u_{\text{cent}} = n_{\text{cent}}/n_0$ and energy densities ε_c for nucleons-only (np) star and for stars with further inclusion of antikaons (npK^-) rotating at Kepler periods P_K are listed below. Results at different values of antikaon optical potential depths $U_{\bar{K}}(n_0)$ (in MeV) at the saturation density are recorded here. The values in parentheses correspond to non-rotating neutron stars.

EoS	$U_{\bar{K}}(n_0)$	$P_K(ms)$	u_{cent}	$\varepsilon_c(10^{15}g/cm^3)$	M_{max}/M_{\odot}	$R(km)$
np	—	0.66	6.40 (7.00)	2.15 (2.43)	2.371 (2.019)	14.84 (11.02)
npK^-	-100	0.80	5.33 (6.12)	1.66 (1.96)	2.189 (1.817)	16.67 (11.98)
	-120	0.91	4.62 (5.20)	1.38 (1.58)	2.005 (1.642)	17.73 (12.62)
	-140	1.06	3.99 (4.56)	1.15 (1.33)	1.648 (1.343)	18.51 (12.98)

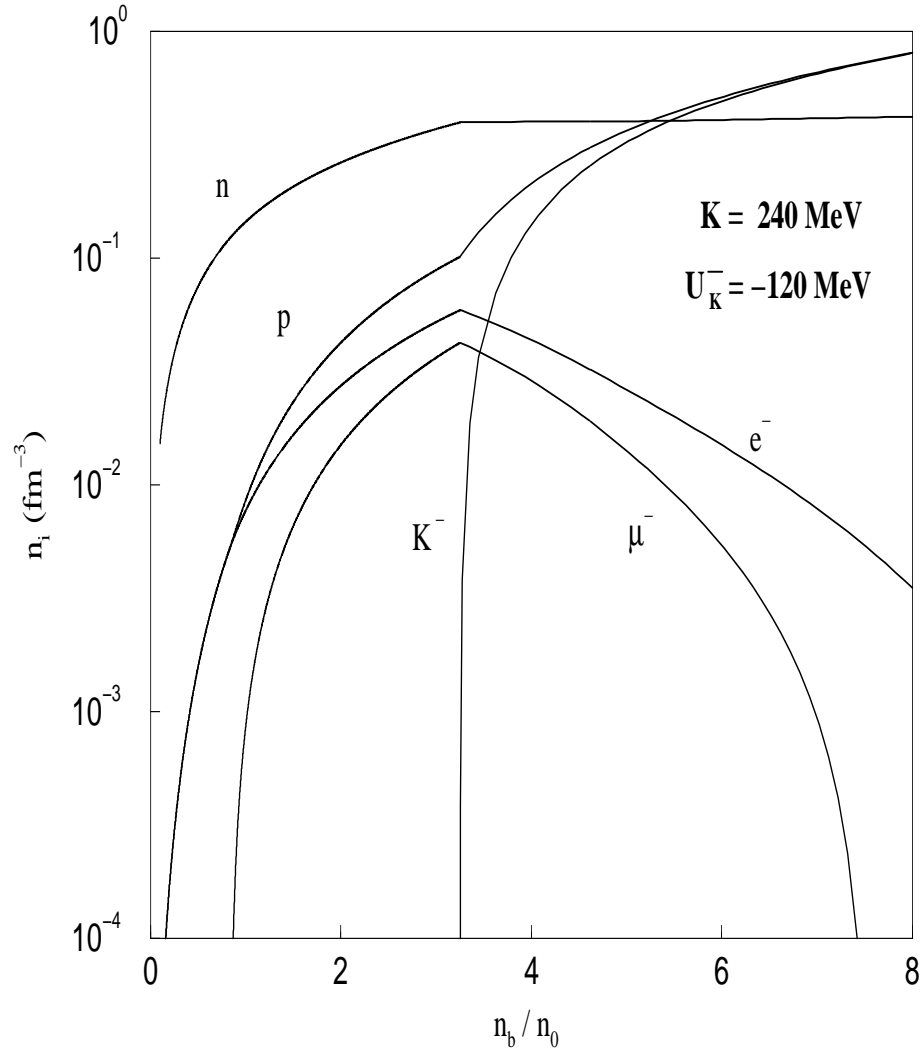


Fig. 1. Particles abundances are plotted with normalised baryon density for antikaon optical potential depths at normal nuclear matter density $U_{\bar{K}}(n_0) = -120 \text{ MeV}$.

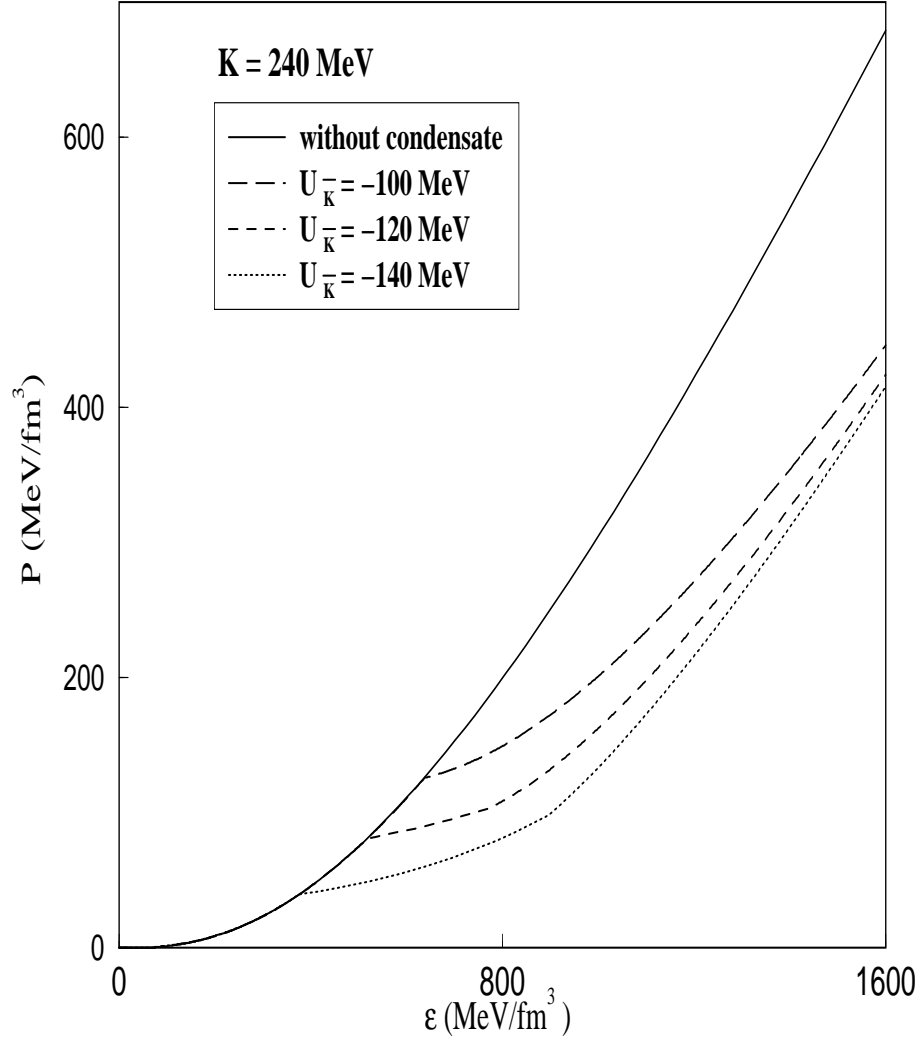


Fig. 2. The equation of state, pressure P vs energy density ϵ , for nucleons-only matter with and without K^- condensate. The results including the condensate are for antikaon optical potential depths at normal nuclear matter density $U_{\bar{K}}(n_0) = -100, -120, -140$ MeV.

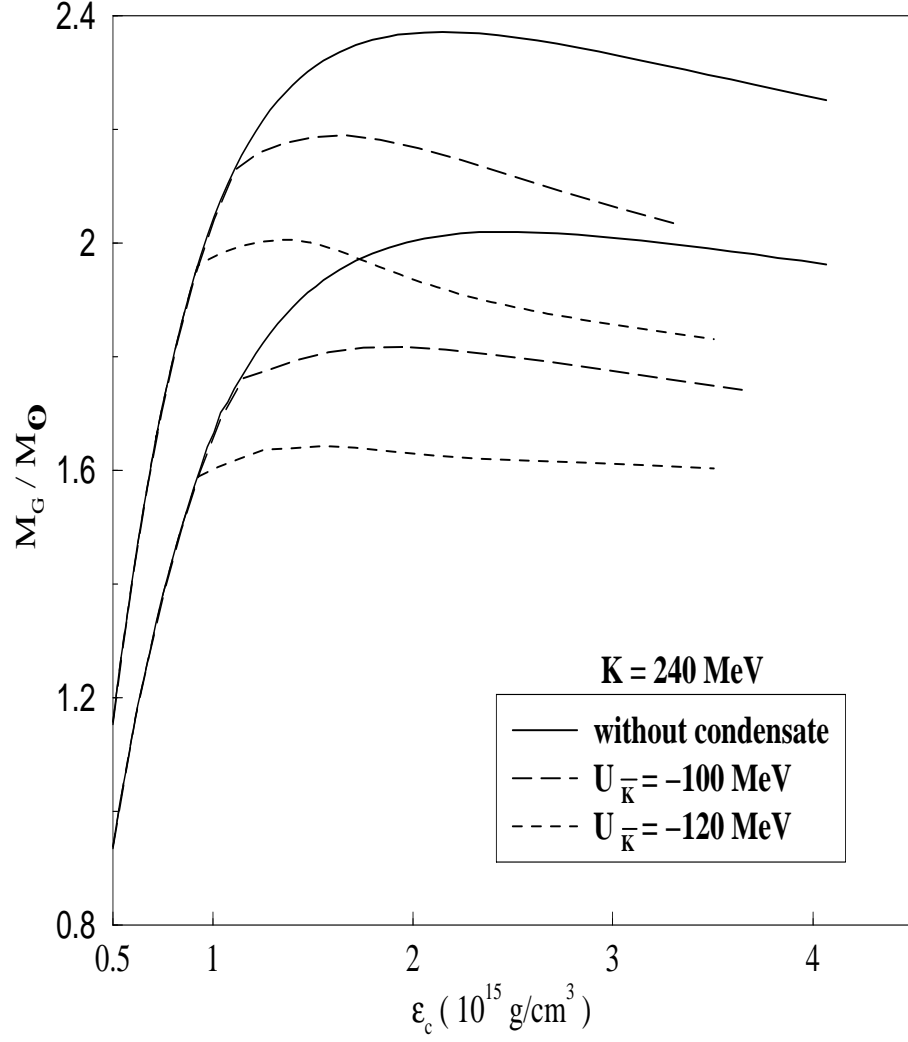


Fig. 3. The gravitational mass for non-rotating sequence as well as mass shedding limit sequence of rotating neutron stars are plotted with central energy density for the equations of state shown in Fig. 2. Different lines have same meaning as in Fig. 2.

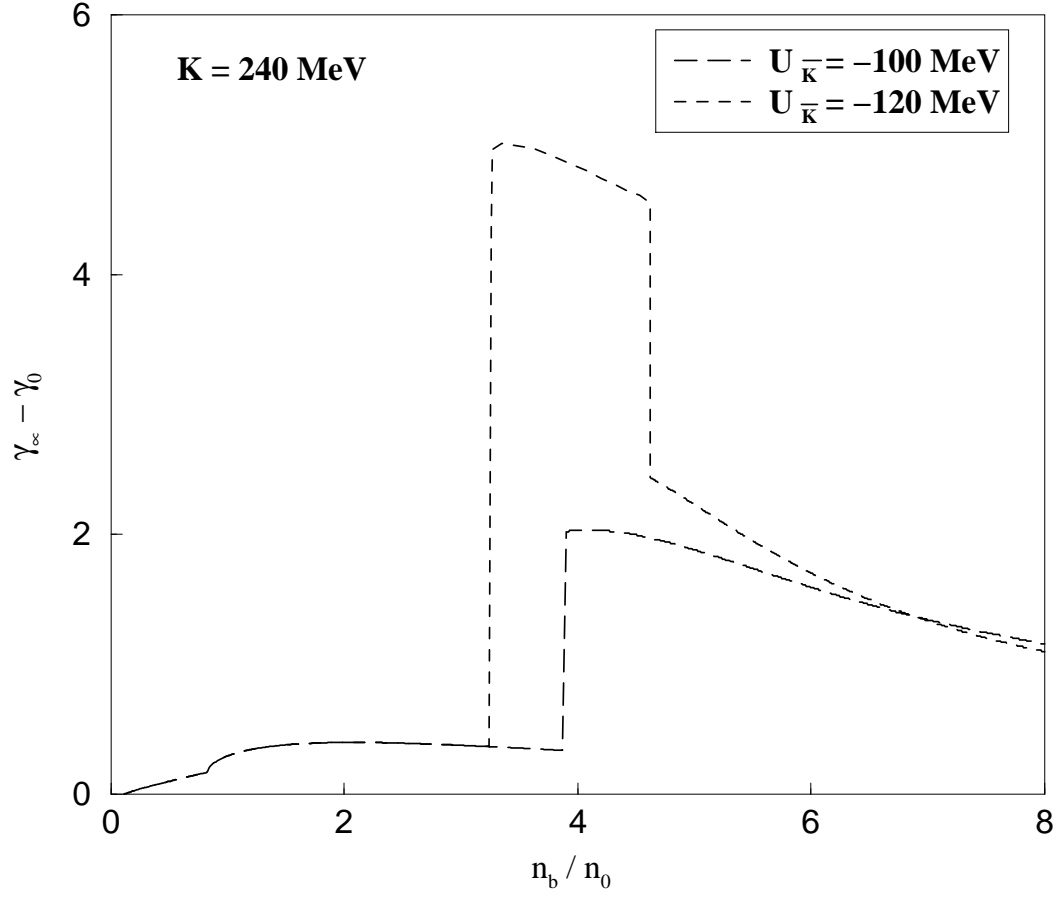


Fig. 4. The difference of adiabatic indices, $\gamma_\infty - \gamma_0$, is shown as a function of normalised baryon density for EoS including K^- condensate with antikaon optical potential depths at normal nuclear matter density $U_{\bar{K}}(n_0) = -100, -120$ MeV.

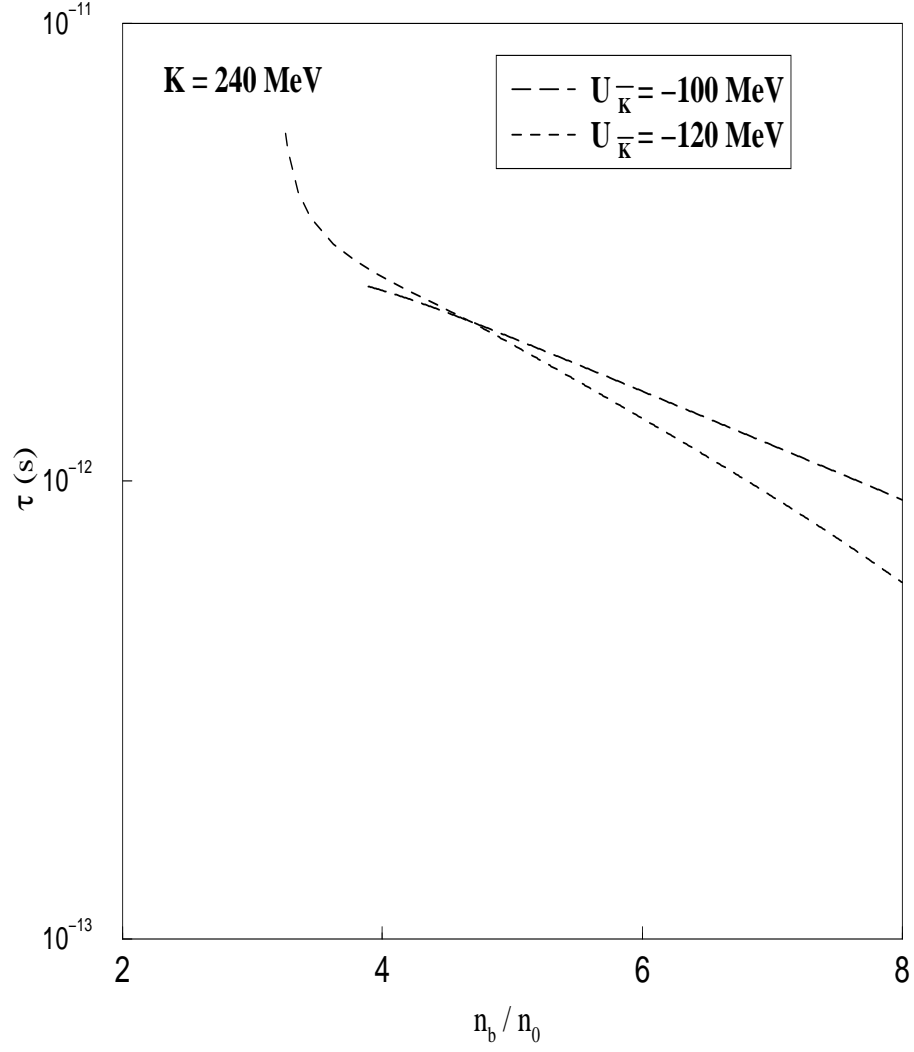


Fig. 5. Relaxation time is plotted with normalised baryon density for the non-leptonic process (21) and antikaon optical potential depths at normal nuclear matter density $U_{\bar{K}}(n_0) = -100, -120$ MeV.

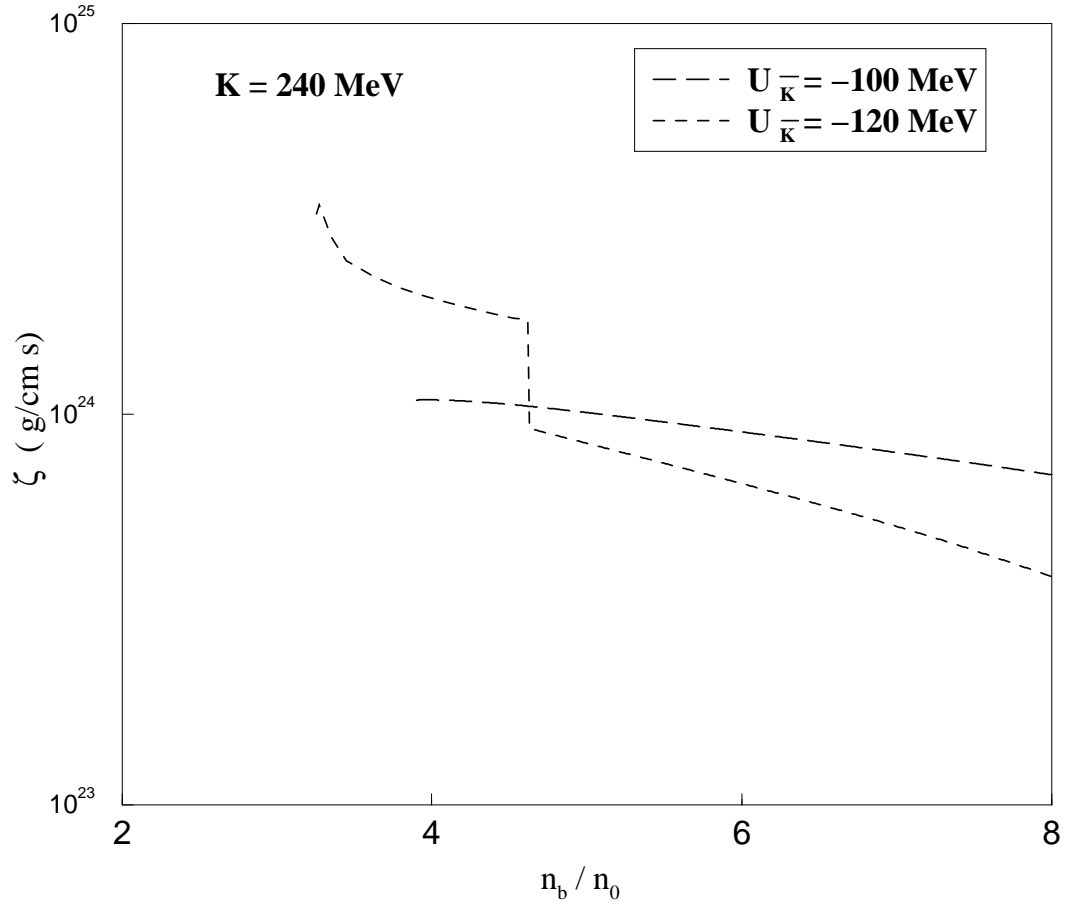


Fig. 6. Bulk viscosity coefficient is exhibited as a function of normalised baryon density for the process (21) and antikaon optical potential depths at normal nuclear matter density $U_{\bar{K}}(n_0) = -100, -120 \text{ MeV}$.

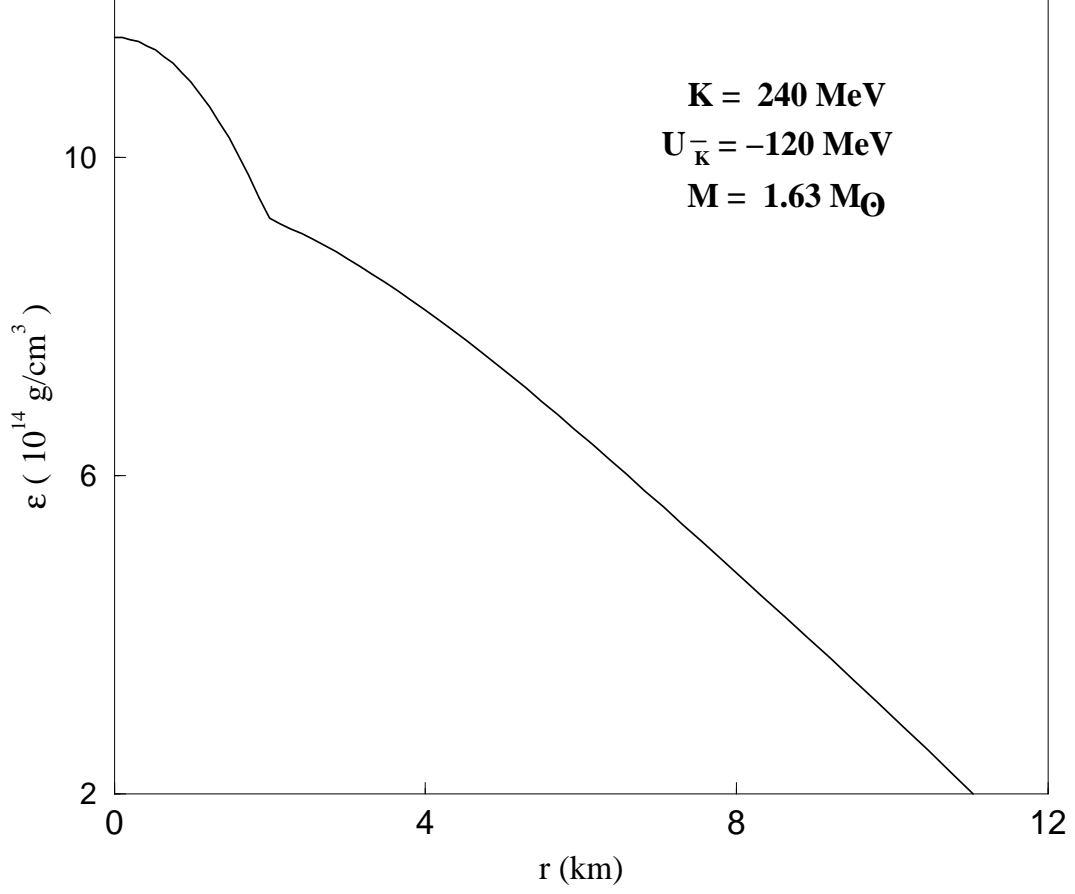


Fig. 7. Energy density profile is shown with equatorial distance for a rotating neutron star of mass $1.63 M_{\odot}$ corresponding to the EoS with antikaon optical potential depth at normal nuclear matter density $U_{\bar{K}}(n_0) = -120 \text{ MeV}$.

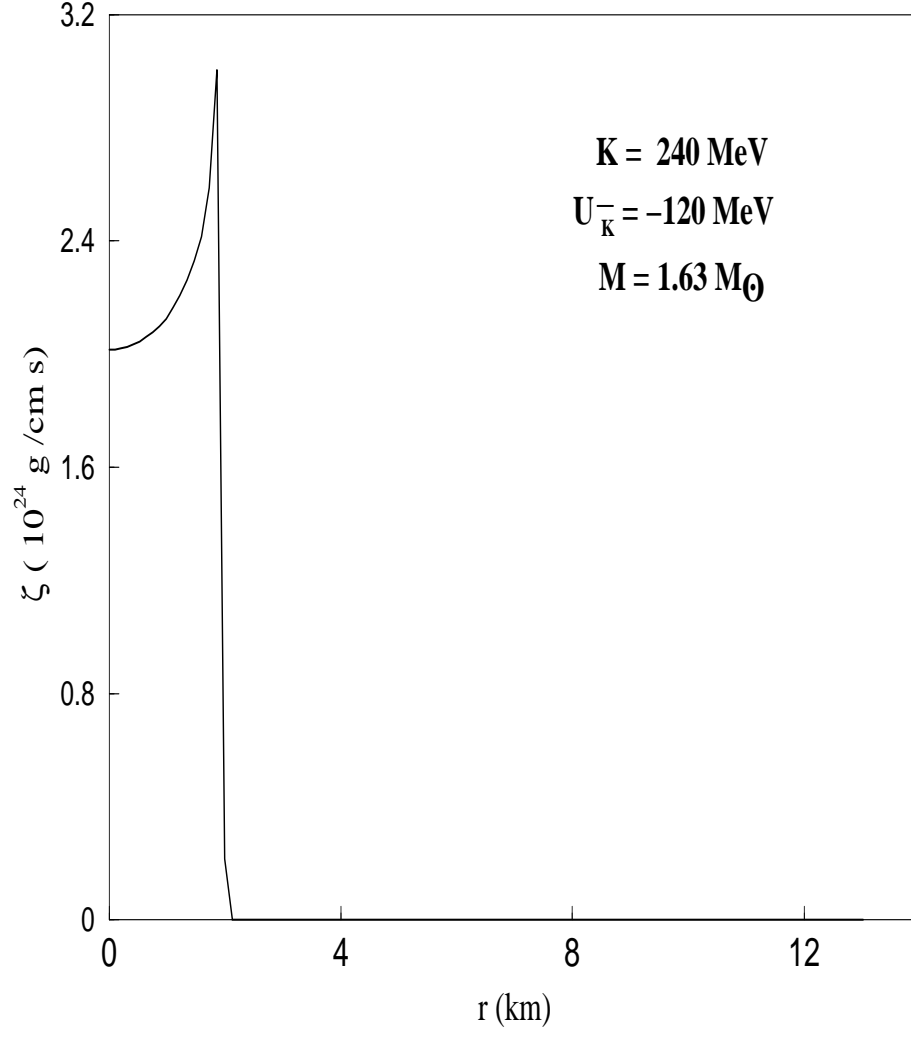


Fig. 8. Bulk viscosity profile is shown with equatorial distance for a rotating neutron star of mass $1.63 M_{\odot}$. The antikaon optical potential depth is same as in Fig. 7.

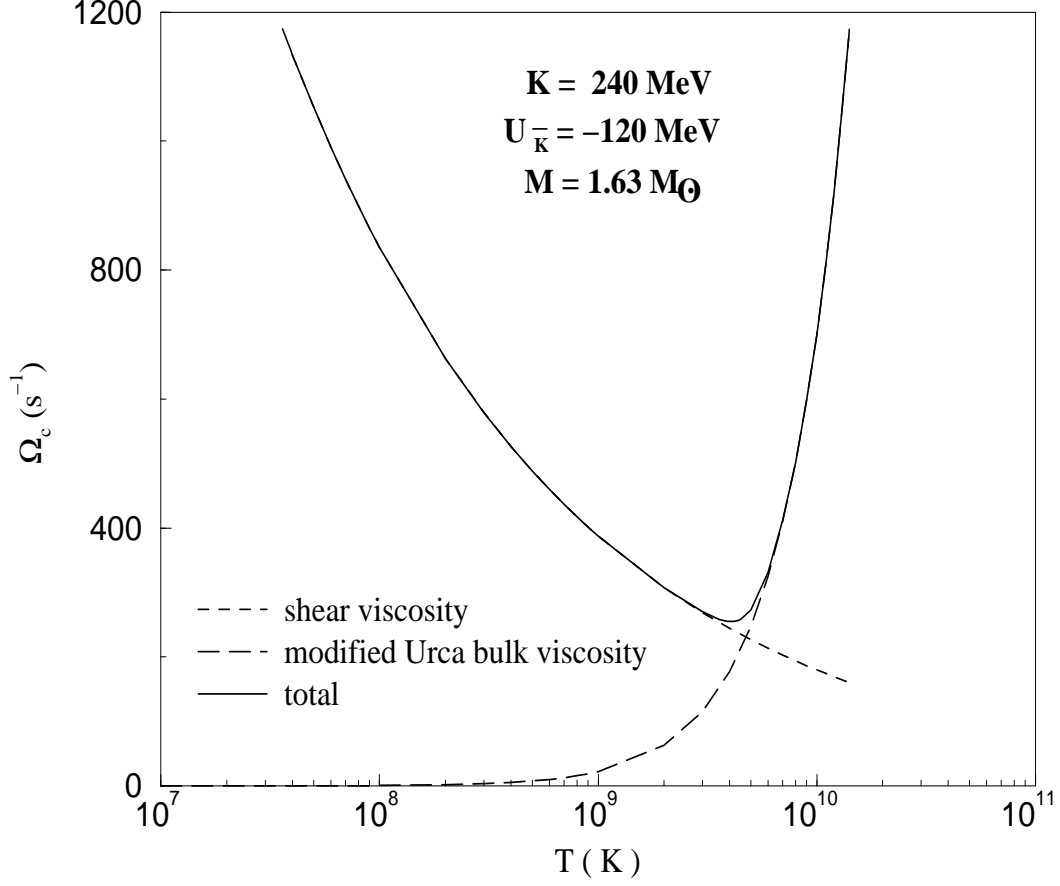


Fig. 9. Critical angular velocity for $1.63 M_{\odot}$ neutron star is plotted as a function of temperature. The antikaon optical potential depth is same as in Fig. 7. The solid line denotes the angular velocity curve when all viscous processes are included. The contributions from the modified Urca bulk viscosity and shear viscosity are shown by long and short dashed lines which merge with the solid line at higher and lower temperatures respectively.